Energy Equip. Sys. / Vol. 8/No. 3/Sep. 2020/ 297-306

ENERGY EQUIPSYS

Energy Equipment and Systems

http://energyequipsys.ut.ac.ir
www.energyequipsys.com

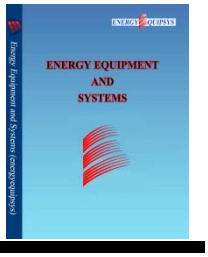

Simulation of an airfoil with a deformable flap applicable in wind turbine structural load reduction

Authors

Majid Ebrahimi [a]
Farzad A. Shirazi [a*]
Kobra Gharali [a]

[a] School of Mechanical Engineering, College of Engineering, University of Tehran, Tehran, Iran

Article history:

Received : 10 June 2019
Accepted : 22 September 2019

ABSTRACT

Flow over an airfoil equipped with Deformable Trailing Edge Flap (DTEF) has been numerically studied in a two-dimensional steady-state condition with various angles of attack. The airfoil is NACA 64-418, and the flap angle is defined by changing camber-line geometry at 10% chord length from the trailing edge. It has been shown that the direction of the flap deflection has significant impacts on aerodynamic behaviors, which provides an extra means to adjust wind turbine structural loads. Simulations have been conducted with aerodynamic-aeroelastic FAST code in the form of an open-loop control scheme to determine the DTEF's performance in a wind turbine. The wind turbine behavior has been plotted and compared for various flap angles. The load-variation ranges of the wind turbine have been identified, which help determine their sensitivity to flap changes. Finally, an open-loop control circuit is aimed at reducing the amplitude of oscillations of the blade root flapwise bending moment.

Keywords: Trailing-Edge Flap; Aerodynamics; Wind Turbine; Smart Rotor.

1. Introduction

Today, due to environmental crises, the use of renewable energy has increased significantly. Wind energy is the type that has attracted much attention due to its cleanness. This has led to a plethora of research on wind turbines trying to reduce the ultimate cost for each kWh generated.

Smart rotor blade technology can be considered as a growing technology in this field. Having used that, the aerodynamic load can be controlled locally. Adding a flap to a section of the blade is a well-known method for changing the aerodynamic pressure distribution around the section. This can result in faster response to triggers and less loads on wind turbine blades and structure.

In recent decades, several studies have been performed on the trailing edge flap and its design and optimization [1-4]. Fuglsang [5] worked on how to obtain 2D airfoil data in the LM Glassfiber wind tunnel. The experiment was conducted on two airfoils with different chords, but the same shapes to investigate the effects of model size on wall correction. Timmer et al. [6] tested NACA 63 and 64 6-series airfoils in Low Turbulence Pressure Tunnel (LTPT) for various parameters and analyzed their aerodynamic characteristics in high Reynolds numbers. In 2010, an experiment was conducted on Risø-B1-18 airfoil with an Active Trailing Edge Flap (ATEF), and the results were presented [7]. ATEF was 9% of the total chord and manufactured of piezoelectric actuators connected to a non-deformable trailing edge flap. Madsen [8] presented the development

* Corresponding author: Farzad A. Shirazi
School of Mechanical Engineering, University of Tehran, Tehran, Iran
Email: fshirazi@ut.ac.ir

of a Controllable Rubber Trailing Edge Flap (CRTEF) for a wind turbine blade. The flap can be deflected by controlling the pressure in suitable designed reinforced voids within the elastic flap. Several prototypes with a chord of 150 mm have been manufactured and tested and mounted on a 1.9 m long airfoil section model with a chord of 1 m for a test in a wind tunnel. A maximum delta CL of about 0.2 was measured in the wind tunnel tests.

Several active controller design research on smart rotors has been conducted to lowering the fatigue and ultimate load affected on the wind turbines [9]. In 2012, Bergami et al. [10] used cyclic pitch control and flap method in order to reduce the fatigue loads on the blade root flapwise bending moment. They observed reductions of nearly 75% in fatigue loads for cyclic pitch control (CPC), whereas cyclic flap control returns a lower reduction, approximately 70%. In another study [11], they have tried to reduce the blade root flapwise bending moment loads by means of a linear-quadratic (LQ) controller. Having used an active flap control, the extreme loads dropped about 13%.
Sun et al. [12] designed a PID controller just for active flap control to reduce the structural loads. They used aero-hydro-servo-elastic nonlinear FAST code to demonstrate the performance of the controller. Finally, the results showed that the deflection of the blades' tips and the blade root flapwise bending moment loads decreased by 24% and 19%, respectively. Furthermore, Henriksen et al. [13] used a Model Predictive Controller

(MPC) and controlled adaptive trailing edge flap (ATEF) through which a 30% decrease of the load was obtained. Wingerden et al. [14] conducted an experiment to study the smart rotor in order to reduce the potential load. They placed TEF on a two-bladed wind turbine and tested in the wind tunnel of Delft University of Technology's Open Jet Facility (OJF). The active part of TEF consisted of Thunder TH-6R. The sensors were also built of macro fiber composite and mounted in the root and measured the strain associated with the first flapwise bending mode. They used the combination of feedback and feedforward scheme to control. The MIMO H_∞ feedback controller was used to reduce stochastic disturbances. Finally, by using this control scheme, the load signal variance reduced by 90%. A full-scale experiment was conducted on a Vestas V27 wind turbine by Castaignet [15]. V27 is a 225 kW and 27m rotor diameter wind turbine located in DTU and Risφ campus. By using the MPC scheme, a 14% decrease was observed in the blade root flapwise moment.

In order to design controllers for wind turbines with smart rotors, including Deformable Trailing-Edge Flaps (DTEFs), it is necessary to obtain models that can predict the DTEF behavior in different operating conditions. The first step in this regard would be 2D simulations of airfoils with DTEF. In 2005, Troldborg et al. [16] carried out a numerical study on Risø-B1-18 airfoil with trailing edge hinged flap in order to investigate the aerodynamic characteristics. A 2D incompressible RANS solver with the k-ω turbulent model with a fully turbulence flow assumption was used for 1.6 million Reynolds number. They also investigated key parameters such as flap shape, flap size, and oscillation frequency in their study. The flap to airfoil chord ratio was proposed between 0.05 and 0.1.

A comparison between aerodynamic predictions of the aeroelastic code HAWC2 and the Navier-Stokes code EllipSys3D for the 5MW reference wind turbine rotor has been presented by Barlas et al. [17]. The wind turbine was equipped with DTEFs. The EllipSys3D solver is a multi-block finite volume discretization of the incompressible Reynolds Averaged Navier-Stokes (RANS) equations in general curvilinear coordinates. To solve the coupled momentum and pressure-correction equations, the iterative SIMPLE or PISO algorithms have been used. For unsteady simulations, a second-order iterative time-stepping (or dual time stepping) method was used.

Looking at the two primary values, it was revealed that HAWC2 predicted a load reduction of 24.63% and 22.45% in thrust and blade root flap-wise bending moment, and EllipSys3D predicted significantly lower reductions of 14.43% and 17.31%, respectively.

An extension of the Beddoes–Leishman-type dynamic stall model was reported by Andersen et al. [18]. A DTEF was added to the dynamic stall model. The model predicted the unsteady aerodynamic forces and moments on an airfoil section undergoing arbitrary motion in heave, lead-lag, pitch, trailing-edge flapping. The model was compared qualitatively to wind tunnel measurements of a Risø-B1-18 blade section equipped with DTEFs in the form of piezoelectric devices. The dynamic lift in both stalled and attached regions showed good agreement with the measurements performed in the Velux tunnel.

Gaunaa [19] described a potential flow's analytical method for the unsteady 2D force distribution on a variable geometry airfoil undergoing arbitrary motion. In addition to already developed potential flow's analytical expressions for unsteady aerodynamics of thin airfoils, this method added the option for a smooth deflection of the airfoil shape by superposition of chordwise deflection mode shapes.

Bergami et al. [20] conducted numerical research on NACA 64-418 airfoil with DTEF. This simulation was performed with three methods: Reynolds-averaged Navier-Stocks solver, viscous-inviscid interaction method, and engineering dynamic stall model. The aerodynamic coefficient has been calculated for the angle of attack between the attached flow condition and separation. Unsteady dynamics undergoing of pitching harmonic motion and flap harmonic deflection was also investigated. The dynamic characteristics of the unsteady response were predicted with an excellent agreement at the attached flow conditions among the investigated methods, both for airfoil pitching and flap deflection. At high angles of attack, where flow separation occurred, the methods still showed similar overall dynamics, but larger discrepancies were reported, especially for the simpler engineering method.

This study gives an overview of the numerical simulation on a wind turbine airfoil equipped with DTEF using CFD A total of 84 two dimensional steady-state simulations have been conducted in various angles of attack and flap deflections. The 5MW wind turbine of NREL [22] has been selected as a reference. The DTEF aerodynamic behaviors obtained from simulation results will be used as inputs to aero-hydro-servo-elastic FAST code. The rest of the paper is organized as follows. In section 2, the flap geometry is defined. The grid generation, CFD simulation details, and the steady-state flow simulation results are explained in Section 3. Section 4 presents numerical results. Aerodynamic-aeroelastic simulations are discussed in section 5, and section 6 concludes the paper.

2. Flap Geometry

The 2D airfoil model considered in this paper is based on NACA 64-418 airfoil with 2.518 m chord length equipped with a deformable trailing edge flap at 10% of the chord length on the trailing edge (Fig. 1). Positive angles of the flap correspond to downward deflection that increases the lift and vice versa for negative angles of the flap. The flap deflection shape is considered as Bergami's investigation [20]. The camber-line is displaced by a distance of $\Delta y_{camb}=\beta.y_{fl}$, where β is the flap deflection in degree and y_{fl}, is the function that describes the flap deflection shape. The deflection shape is defined as a circular arc starting at 90% of the chord length.

$$\frac{y_{fl}}{c}:\begin{cases} y_{fl}=0 & \text{for } x/c<0.9 \\ y_{fl}=\sqrt{R_c^2-\left(x/c-0.9\right)^2}-R_c & \text{for } x/c\geq 0.9 \end{cases} \quad (1)$$

where the radius of the arc is given by:

$$R_c=\frac{0.1^2+\delta_y^2}{2\delta_y}, \quad (2)$$

$$\delta_y=0.1\tan\left(\beta.\pi/180\right) \quad (3)$$

3. Numerical setup

The details of the reference 5MW wind turbine of NREL [22] has been provided in Table I. It was assumed that the flapped.

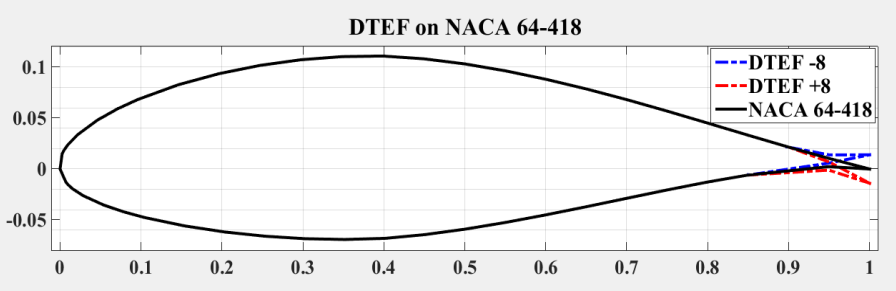

Fig. 1. Flap deflection of ±8˚ on NACA 64-418.

section is located at 67% to 95% of the blade length of the reference wind turbine. Considering the wind speed and the rotational speed of the blades, the Reynolds number of Re=11.26×10^6 has been calculated.

The obtained Reynolds number indicates that the flow around the airfoil is fully turbulent. Hence, the turbulence in the boundary layer is modeled by the k − ω Shear Stress Transport (SST) eddy viscosity model. The turbulence model will be verified later.

A. Grid generation

The type of generated mesh is C-Type. Around 2×105 quadratic cells resulted in a satisfactory independent mesh. The first cell in the boundary layer has a height of 1×10−6 m with y+ of less than 1. The orthogonality of the mesh has been checked. The outer boundaries of the domain were placed approximately eight times of the airfoil chord length away from the airfoil. Figure 2 shows the mesh around the airfoil.

B. Steady-state simulations

All simulations were conducted in a steady-state condition. It should be mentioned that

$$k = \frac{\omega c}{2U_\infty} \quad (4)$$

where, ω is the frequency of the harmonic variations, c is the chord length, and U_∞ indicates the free-stream flow speed. The reduced frequency of less than 0.02 gives the quasi-steady condition, around 0.1 refers to the unsteady condition, and over 0.5 corresponds to the highly unsteady conditions. In this study, chord length is considered 2.518 m, and the flap chord is 10% of it. With the flap frequency of less than 10.5 Hz related to the current study, the quasi-steady condition is satisfied.

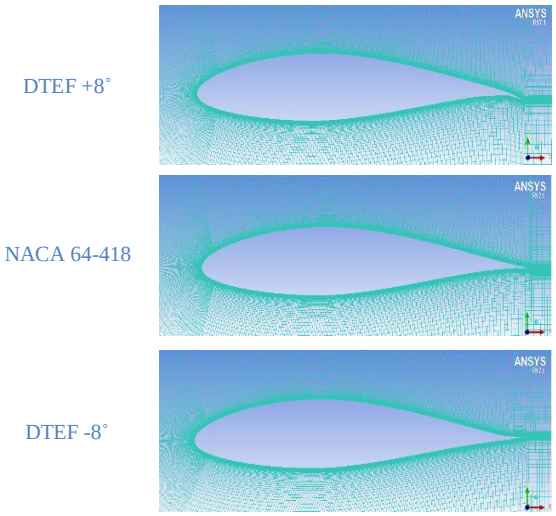

Fig.2. C-type mesh around the airfoil.

Table 1. 5MW Reference wind turbine properties

#	Property	Value
1	Rating	5 MW
2	Control	Variable speed, Collective Pitch
3	Rated Mechanical Power	5.296610 MW
4	Rated Generated Torque	43,099.55 N.m
5	Rotor, Hub Diameter	126 m, 3 m
6	Cut in, Rated, Cut out wind speed	3 m/s, 11.4 m/s, 25 m/s
7	Cut in, Rated Rotor Speed	6.9 rpm, 12.1 rpm
8	Blade length	63 m
9	Rated Tip Speed	80 m/s

4. Numerical results

Several computational simulations at Re=11.26×10^6 have been conducted for three angles of DTEF ±8˚ and 0˚ and between 10˚ and 19˚ angle of attack in order to study the aerodynamic response of NACA 64-418 to deformable flap deflection. Figure 3 compares the obtained lift coefficients for zero DTEF with experimental results [6] and X-foil results [22].

For the linear section, the numerical and experimental results agree well. After stall, X-foil results are not valid, and experimental results show lower lift coefficients. It should be mentioned that the current study has a higher Reynolds number than experimental studies. Therefore, the lift values from the experiments are lower; however, the trends are the same.

Figures 4 and 5 present the effects of flap deflection on aerodynamic loads. Each 8-degree flap deflection makes approximately 0.3 lift coefficient changes. A positive deflection increases and a negative deflection reduces aerodynamic loads, lift and drag coefficients, respectively. The reported aerodynamic results are valid for ±8° variations of DTEF since higher amplitudes can result in different flow patterns around the airfoil.

The lift to drag ratio is represented in Fig.6. The larger the lift and the smaller the drag coefficients, the more effective forces, and torques will act on the wind turbine resulting in more generated power with less structural loads. Figure 6 shows that changing the flap deflection can change the ratio of the lift to drag. In lower angles of attack (AOAs), the ratio varies around 60, but in higher AOAs above 12 degrees, the variations are quite low, and different flap deflections result in similar results. This point is important in flap control because, in low AOAs, the lift can be raised while the drag is fixed, but in higher AOAs increasing the lift leads to higher drag and loads. In fact, this subject leads to smart flap deflection control in order to reduce structural loads.

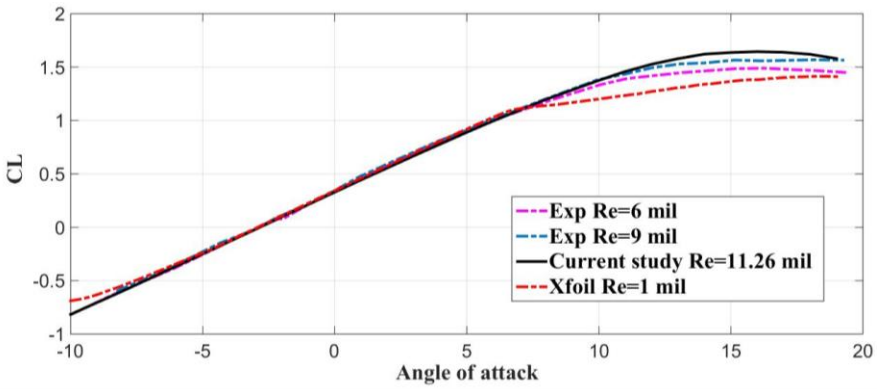

Fig.3. Comparison of computational lift coefficients with exprimental results and X-foil for NACA 64-418 airfoil, zero deflection.

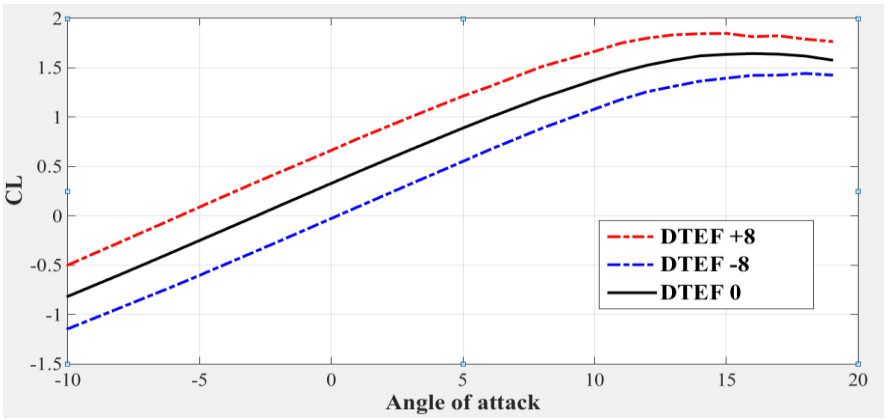

Fig. 4. Effects of flap deflection on lift coefficient of NACA 64-418.

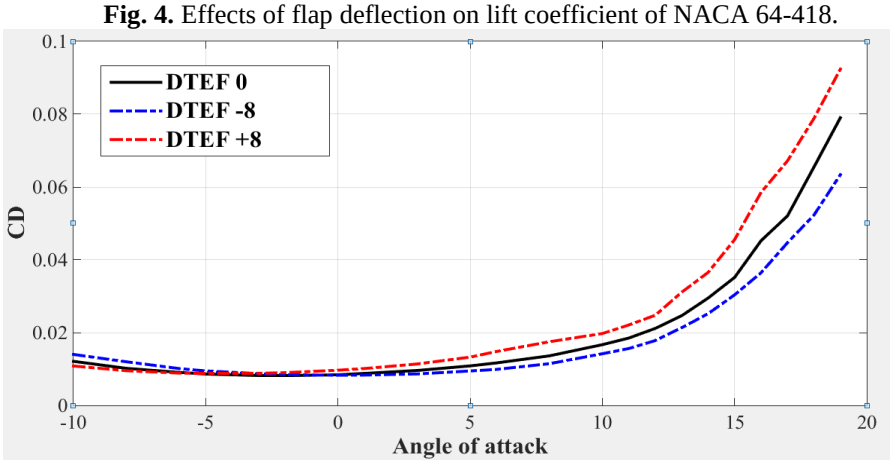

Fig. 5. Effects of flap deflection on drag coefficient of NACA 64-418.

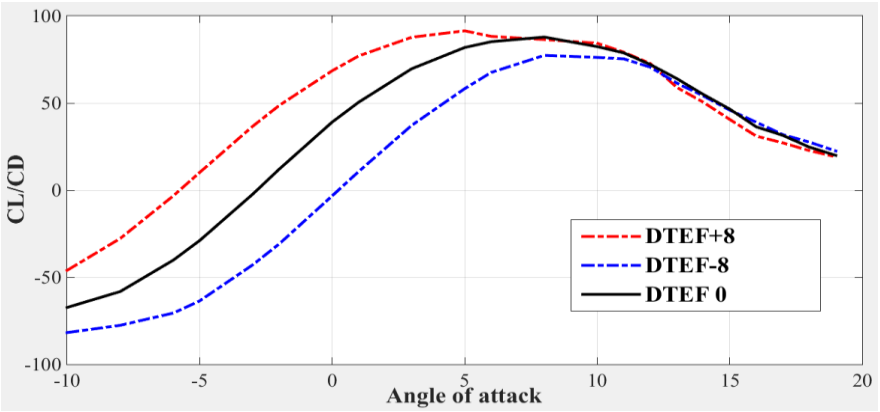

Fig. 6. Effects of flap deflection on the lift to drag coefficient ratio of NACA 64-418 airfoil.

5. Aerodynamic-aeroelastic simulations

The simulations of NREL 5-MW reference wind turbine with DTEFs were conducted by FAST to analyze the time response of the entire wind turbine. FAST is a widely used aerodynamic-aeroelastic analysis code for wind turbines. The FAST (Fatigue, Aerodynamics, Structures and Turbulence) code code is a comprehensive aeroelastic simulator capable of predicting both extreme and fatigue loads [21].

The aerodynamic sub-model uses wind-inflow data and solves for rotor-wake and blade-element aerodynamic loads, including dynamic stall loads. The control module simulates control logics, sensors, and actuators of the blade pitch, generator-torque, and other devices, but by default, it does not have the capability of DTEF's control. The

aeroelastic sub-model applies the aerodynamic loads, gravitational loads, control, and electrical system reactions on the blades and structure. Also, it considers the elasticity of the rotor, drivetrain, and supports the structure.

In this study, In order to implement the dynamic control process, the FAST code should in to account for DTEF control action and the resulting change of aerodynamic properties. This was achieved by Multi-Table function in the FAST code. The FAST code allows users to input a multiset of aerodynamic properties associated with a set of corresponding Multi-Table identification variables. In the default setting, the Multi-Table variable represents the Reynolds number. At each time step, once the actual Reynolds number is calculated, the actual aerodynamic properties are linearly interpolated between available values to obtain desired Reynolds number. Here, this feature was used for applying effects of DTES for -8, 0, +8 flap deflections, and interpolation was conducted for other flap deflections in the range. The control logic was coded in Matlab Simulink interface in order to adjust flap angles dynamically. Finally, the FAST S_function block in Matlab Simulink was built with DTEF controllability (Fig. 7).

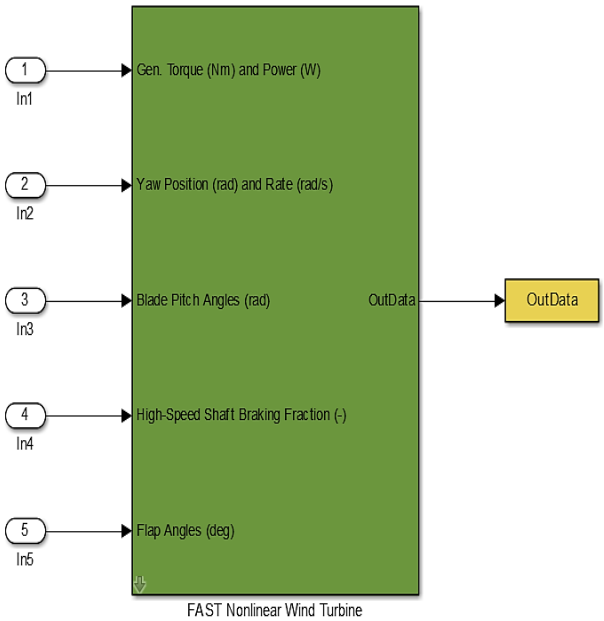

Fig. 7. Modified FAST S_Function block in Simulink in order to DTEF control

The generator torque, power demand, yaw control, blade pitch control, high-speed shaft brake inputs were available, and three input flap angles have been added, newly. In fact, DTEFs can drastically change the loads exerted on wind turbines, and this can provide a powerful tool for load control.

Figure 8 shows the range of loads, accelerations, and deflections when changing the DTEF from -8 to +8 degrees. This simulation was also performed in no DTEF mode as a baseline for comparison. The thrust force, blade root flapwise, and edgewise bending moments are the most sensitive to DTEF variations.

The rotor torque is not sensitive to flap deflection because in region 3, the high-speed shaft torque is kept almost constant, and it fluctuates until it gets to the steady-state condition. The tower top fore-aft and side-side deflections show that by decreasing flap deflection, the oscillation range has been decreased, and by increasing, no significant change was observed. Reducing flap angle to -8 degree has increased the tower fore-aft acceleration amplitude. The tower side-side acceleration amplitude is minimum at -8 degrees flap deflection.

The effect of DTEF variations on wind turbine behavior is presented in Fig. 10. Three DTEF input step functions were applied in order to influence the wind turbine significantly. The simulation was conducted in an equilibrium state with 18 m/s steady-state exponential wind speed. Results show that DTEF control could reduce ultimate and fatigue load damages on blades and structure, significantly. The generator speed changes by changing DTEF angles, as shown in Fig. 10 because of the constant generator torque in the high-speed region. The change in the rotor speed causes fatigue loads on the blades and the structure, which should be considered in the closed-loop control flap.

In recent researches, more attention has been paid to reducing blade root flapwise bending moment [10], [11]. In Fig. 11, an open-loop control scheme has been conducted to reduce blade root flapwise bending moment amplitude with flap angle input step functions, which proves that it is possible to reduce the oscillation range of fatigue and ultimate loads by controlling the angle of the flap.

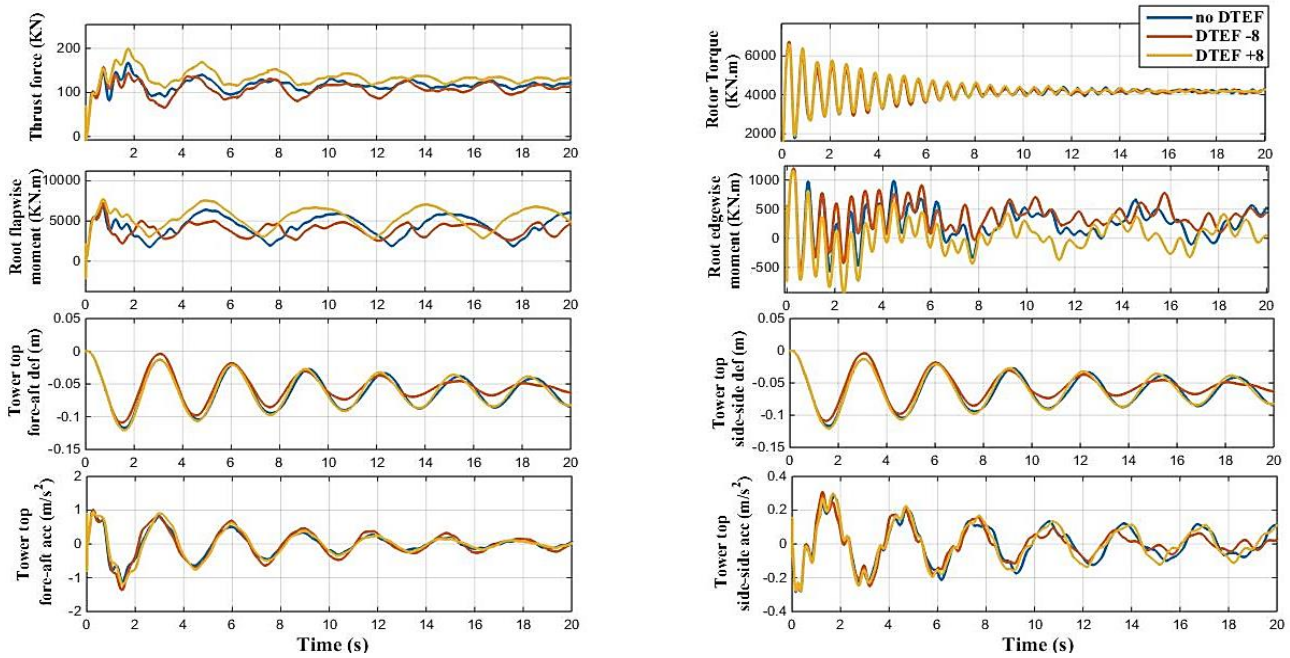

Fig. 8. Load range creatation by DTEF.

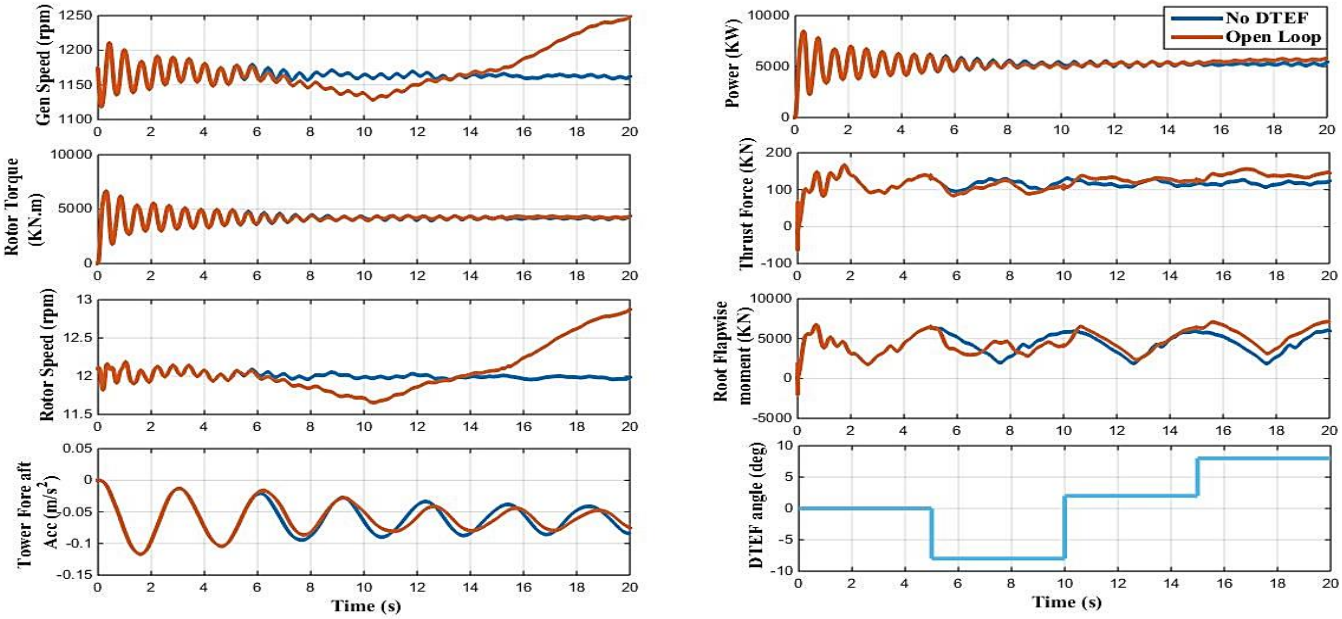

Fig. 9. Effects of DTEF variations on wind turbine behavior

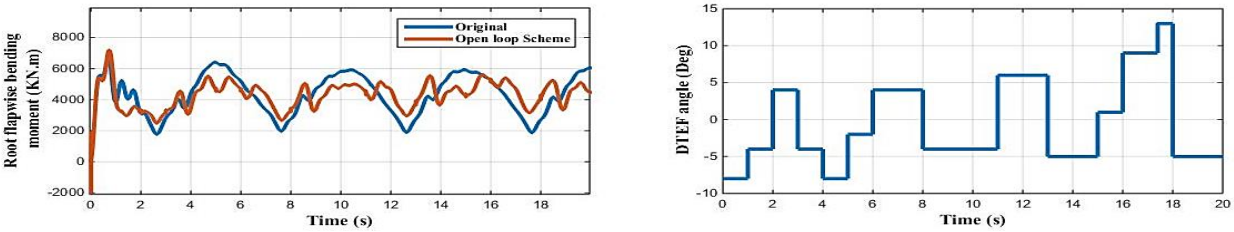

Fig. 10. Effects of DTEF variations on wind turbine behavior

6. Conclusions

In this study, the aerodynamic characteristics of a two-dimensional steady NACA 64-418 wind turbine airfoil with various flap deflections were investigated numerically. It was observed that flap deflections remarkably change aerodynamic lift and drag coefficients and their ratio; by increasing and decreasing the deflection, the coefficients vary accordingly. The airfoil with DTEF was used for the 5MW reference wind turbine blades, and the FAST code was modified to consider DTEFs. The simulations were performed in the FAST code to study the effects of DTEF variations on wind turbine structural behavior. An open-loop simulation was also conducted to show the ability of DTEF to reduce fatigue and ultimate loads. It was revealed that DTEF could provide extra degrees of freedom for wind turbines to adjust the aerodynamic loads.

For future work, an H_∞ robust controller will be designed for flap and pitch control of the 5 MW reference wind turbine and implemented in the FAST code. The control objective will be to reduce the ultimate and fatigue loads on blades and structures.

References

[1] Franco, J. A., Jauregui, J. C., & Toledano-Ayala, M. (2015). Optimizing wind turbine efficiency by deformable structures in smart blades. Journal of Energy Resources Technology, 137(5), 051206.

[2] Andersen, T. L., Madsen, H. A., Barlas, T. K., Mortensen, U. A., & Andersen, P. B. (2015). Design, manufacturing and testing of Controllable Rubber Trailing Edge Flaps.

[3] Berg, D., Berg, J., White, J., Resor, B., & Rumsey, M. (2011). Design, fabrication, assembly and initial testing of a SMART rotor. In 49th AIAA Aerospace Sciences Meeting including the New Horizons Forum and Aerospace Exposition (p. 636).

[4] McWilliam, M., Barlas, A., Madsen, H. A., & Zahle, F. (2018). Aero-elasticWind Turbine Design with Active Flaps for AEP Maximization. Wind Energy Science Discussions, 3, 231-241.

[5] Fuglsang, P., & Bove, S. (2008). Wind tunnel testing of airfoils involves more than just wall corrections. In EWEC Conference.

[6] Timmer, W. (2009, January). An overview of NACA 6-digit airfoil series characteristics with reference to airfoils for large wind turbine blades. In 47th AIAA aerospace sciences meeting including the new horizons forum and aerospace exposition (p. 268).

[7] Bak, C., Gaunaa, M., Andersen, P. B., Buhl, T., Hansen, P., & Clemmensen, K. (2010). Wind tunnel test on airfoil Risø-B1-18 with an Active Trailing Edge Flap. Wind Energy: An International Journal for Progress and Applications in Wind Power Conversion Technology, 13(2-3), 207-219.

[8] Madsen, H. A., Andersen, P. B., Andersen, T. L., Bak, C., Buhl, T., & Li, N. (2010). The potentials of the controllable rubber trailing edge flap (CRTEF). In 2010 European Wind Energy Conference and Exhibition. European Wind Energy Association (EWEA).

[9] Johnson SJ, Baker JP, van Dam CP, Berg D. An overview of active load control techniques for wind turbines with an emphasis on microtabs. Wind Energy

2010; **13**(2-3): 239–253. doi:10.1002/we.356.

[10] Bergami, L., & Henriksen, L. C. (2012). Cyclic control optimization for a smart rotor. In Proceedings of the 8th PhD Seminar on Wind Energy in Europe.

[11] Bergami, L., & Poulsen, N. K. (2015). A smart rotor configuration with linear quadratic control of adaptive trailing edge flaps for active load alleviation. Wind Energy, 18(4), 625-641.

[12] Sun, X., Dai, Q., Menon, M., & Ponta, F. (2017). Design and simulation of active external trailing-edge flaps for wind turbine blades on load reduction. Journal of Aerospace Engineering, 30(5), 04017062.

[13] Henriksen, L. C., Bergami, L., & Andersen, P. B. (2013). A model based control methodology combining blade pitch and adaptive trailing edge flaps in a common framework. EWEA Annual Event, Vienna, Austria.

[14] Van Wingerden, J. W., Hulskamp, A., Barlas, T., Houtzager, I., Bersee, H., van Kuik, G., & Verhaegen, M. (2011). Two-degree-of-freedom active vibration control of a prototyped "smart" rotor. IEEE transactions on control systems technology, 19(2), 284-296.

[15] Castaignet, D., Barlas, T., Buhl, T., Poulsen, N. K., Wedel-Heinen, J. J., Olesen, N. A. & Kim, T. (2014). Full-scale test of trailing edge flaps on a Vestas V27 wind turbine: active load reduction and system identification. Wind Energy, 17(4), 549-564.

[16] Troldborg, N. (2005). Computational study of the Risø-B1-18 airfoil with a hinged flap providing variable trailing edge geometry. Wind Engineering, 29(2), 89-113.

[17] Barlas, T. K., Zahle, F., Sørensen, N. N., Gaunaa, M., & Bergami, L. (2012). Simulations of a rotor with active deformable trailing edge flaps in half-wake inflow: Comparison of EllipSys 3D with HAWC2. In EWEA 2012-European Wind Energy Conference & Exhibition. European Wind Energy Association (EWEA).

[18] Andersen, P. B., Gaunaa, M., Bak, C., & Hansen, M. H. (2009). A dynamic stall model for airfoils with deformable trailing edges. Wind Energy: An International Journal for Progress and Applications in Wind Power Conversion Technology, 12(8), 734-751.

[19] Gaunaa, M. (2006). Unsteady 2D potential-flow forces on a thin variable geometry airfoil undergoing arbitrary motion.

[20] Bergami, L., Riziotis, V. A., & Gaunaa, M. (2015). Aerodynamic response of an airfoil section undergoing pitch motion and trailing edge flap deflection: a comparison of simulation methods. Wind Energy, 18(7), 1273-1290.

[21] Jonkman, J., Butterfield, S., Musial, W., & Scott, G. (2009). Definition of a 5-MW reference wind turbine for offshore system development (No. NREL/TP-500-38060). National Renewable Energy Lab. (NREL), Golden, CO (United States).

[22] airfoil tools. 2018. airfoil tools. [ONLINE] Available at: http://airfoiltools.com/. [Accessed 1 November 2018].